# An Improved Conscan Algorithm Based on a Kalman Filter

D. B. Eldred
Guidance and Control Section

*Conscan is commonly used by DSN antennas to allow adaptive tracking of a target whose position is not precisely known. This article describes an algorithm that is based on a Kalman filter and is proposed to replace the existing fast Fourier transform–based (FFT-based) algorithm for conscan. Advantages of this algorithm include better pointing accuracy, continuous update information, and accommodation of missing data. Additionally, a strategy for adaptive selection of the conscan radius is proposed. The performance of the algorithm is illustrated through computer simulations and compared to the FFT algorithm. The results show that the Kalman filter algorithm is consistently superior.*

## I. Introduction

The objective of conscan is to improve the estimate of the target location; the target location is defined as the direction of maximum carrier power as received on the ground. During conscan, the antenna is rotated in a circle about a point we call the conscan center at a constant rate $\omega$. Figure 1 shows the variables used in the analysis.

Without loss of generality the origin is placed at the conscan center. We define $\mathbf{x} \equiv \mathbf{x}(t)$ as the 2-vector which specifies what we seek to estimate: the unknown actual target at time $t$, and we define $\hat{\mathbf{x}} \equiv \hat{\mathbf{x}}(t)$ as the estimate of the target's location. We assume that discrete measurements are taken at times $t = t_i$. Let the subscript "$i$" denote a quantity taken at time $t_i$; for example, $\mathbf{x}_i \equiv \mathbf{x}(t_i)$. Lack of the "$i$" subscript implies that the affected quantity is constant over a conscan period. We refer to $\mathbf{x}_i$ as the state of the system, and thus $\hat{\mathbf{x}}_i$ is the state estimate. The known instantaneous location of the antenna boresight is defined by $\mathbf{x}_{ai}$, which during conscan is given by

$$\mathbf{x}_{ai} = \begin{bmatrix} R\cos(\omega t_i) \\ R\sin(\omega t_i) \end{bmatrix} \tag{1}$$

Here, $R$ is referred to as the conscan radius, and $\omega$ is the conscan frequency.

The output of the antenna receiver is the carrier power $P_{0i}$. Assuming a circularly symmetric antenna gain func-

tion, the carrier power can be approximated as a quadratic function of the offset angle:[1]

$$P_{ci} = P_{0i}\left(1 - \mu\frac{\beta_i^2}{h^2}\right) + \eta_i \tag{2}$$

where $P_{0i}$ is the maximum carrier power which occurs when the antenna is pointed directly at the target, $h$ is the antenna half-power beamwidth, $\mu = 4\ln(2)$, $\beta_i$ is the offset angle between the antenna boresight and the target, and $\eta_i$ is the signal noise, or error. We assume that the signal noise is random with zero mean and is Gaussian distributed with a standard deviation of $\sigma_\eta$. From Fig. 1, we have

$$\beta_i = \sqrt{(\mathbf{x}_i - \mathbf{x}_{ai})^\mathsf{T}(\mathbf{x}_i - \mathbf{x}_{ai})} \tag{3}$$

and thus

$$P_{ci}(\mathbf{x}_i) = P_{0i}\left(1 - \frac{\mu}{h^2}(\mathbf{x}_i - \mathbf{x}_{ai})^\mathsf{T}(\mathbf{x}_i - \mathbf{x}_{ai})\right) + \eta_i \tag{4}$$

If we assume that $P_{0i} = P_0$ and $\mathbf{x}_i = \mathbf{x}$ are constant throughout a conscan period, then from Eq. (1) it is easily shown that the ensemble average of the carrier power over the conscan period is approximately

$$\langle P_{ci}\rangle \approx P_0\left(1 - \frac{\mu}{h^2}(\mathbf{x}^\mathsf{T}\mathbf{x} + R^2)\right) \tag{5}$$

Subtracting Eq. (5) from Eq. (4) yields

$$P_{ci}(\mathbf{x}_i) - \langle P_{ci}\rangle \approx \frac{2P_0\mu}{h^2}\mathbf{x}_{ai}^\mathsf{T}\mathbf{x}_i + \eta_i \tag{6}$$

Equation (6) constitutes the measurement equation for the purposes of the estimators. It is important to note that the measurement equation is linear with respect to the unknown state $\mathbf{x}_i$, as this makes it possible to apply linear estimation theory to estimate $\mathbf{x}_i$.

We define $\mathbf{z}_i$ as

$$\mathbf{z}_i \equiv P_{ci}(\mathbf{x}_i) - \langle P_{ci}\rangle \tag{7}$$

and thus

$$\mathbf{z}_i = \frac{2P_0\mu}{h^2}\mathbf{x}_{ai}^\mathsf{T}\mathbf{x}_i + \eta_i \tag{8}$$

In the subsequent analysis, we refer to $\mathbf{z}_i$ as our *measurement.*

## II. FFT Estimator

A brief discussion of the existing fast Fourier transform (FFT) estimator is given below so that it can be compared to the Kalman filter estimator. We assume that $P_{0i} = P_0$ and $\mathbf{x}_i = \mathbf{x}$ are constant over a conscan period. Multiplying Eq. (8) by $\mathbf{x}_{ai}$ and averaging both sides over a conscan period yields, after some algebra,

$$\langle \mathbf{z}_i\mathbf{x}_{ai}\rangle = \frac{P_0\mu R^2}{h^2}\mathbf{x} + \langle \eta_i\mathbf{x}_{ai}\rangle \tag{9}$$

Utilizing the fact that $\eta_i$ is assumed to be zero mean, we obtain an estimate for the state:

$$\hat{\mathbf{x}} = \frac{h^2\langle \mathbf{z}_i\mathbf{x}_{ai}\rangle}{P_0\mu R^2} \tag{10}$$

We define $\mathbf{M}$ to be the covariance of the state estimate:

$$\mathbf{M} \equiv E\left((\hat{\mathbf{x}}_i - \mathbf{x})(\hat{\mathbf{x}}_i - \mathbf{x})^\mathsf{T}\right) \tag{11}$$

where $E$ denotes expectation, or ensemble average. After further manipulation it can be shown that

$$\mathbf{M} = \frac{h^4\sigma_\eta^2}{2P_0^2\mu^2R^2n}\mathbf{I} \tag{12}$$

where $\mathbf{I}$ is the 2 × 2 identity matrix and $n$ is the number of samples taken over a single conscan period. This result is consistent with results described elsewhere.[2]

In practice, an FFT is used to estimate $\mathbf{x}$ [1]; this yields the same result as Eq. (10) but also yields harmonics above the fundamental frequency. Hence, we call this the FFT algorithm. Use of an FFT imposes several constraints on the algorithm: $n$ must be an integer power of 2; there must be no missing measurements; and the measurements must be evenly spaced in time. Theoretically, failure in

[1] L. Alvarez, "Open Loop Conscan Pointing Error Estimation Accuracy at Ka-band," JPL Interoffice Memorandum 3328-93-044 (internal document), Jet Propulsion Laboratory, Pasadena, California, July 8, 1993.

[2] Ibid.

the estimator can be detected by the presence of significant amplitudes in the harmonics above the fundamental frequency, but in practice, detection of the harmonics above the fundamental frequency has been only partially implemented, partly because it is readily apparent when conscan has failed.

## III. Kalman Filter Estimator

A detailed general description of a Kalman filter is given in [2]. However, square root algorithms in which the Cholesky factors of the covariance matrix are propagated are widely recognized to have superior numerical properties, and hence we implement the square root covariance filter described in [3]. We assume that between time intervals $t_i$ and $t_{i+1}$, $\mathbf{x}_i$ drifts according to

$$\mathbf{x}_{i+1} = \mathbf{x}_i + \mathbf{n}_i \tag{13}$$

where $\mathbf{n}_i$ is a random 2-vector with covariance $\mathbf{Q} \equiv E(\mathbf{n}_i\mathbf{n}_i^\mathsf{T})$. We assume that at time $t_i$ the state estimate is known with covariance $\mathbf{M}_i \equiv E\left((\hat{\mathbf{x}}_i - \mathbf{x}_i)(\hat{\mathbf{x}}_i - \mathbf{x}_i)^\mathsf{T}\right)$. Our measurements take the form

$$\mathbf{z}_i = \mathbf{H}_i\mathbf{x}_i + \mathbf{v}_i \tag{14}$$

where $\mathbf{v}_i$ is a random vector with zero mean and whose covariance is given by $\mathbf{R} \equiv E\left(\mathbf{v}_i\mathbf{v}_i^\mathsf{T}\right)$. From Eq. (8), we can make the identifications

$$\begin{aligned} \mathbf{H}_i &= \frac{2P_0\mu}{h^2}\mathbf{x}_{ai}^\mathsf{T} \\ \mathbf{v}_i &= \eta_i \\ \mathbf{R} &= \sigma_\eta^2 \end{aligned} \tag{15}$$

With these preliminaries completed, we are ready to construct the Kalman filter estimator, which requires execution of the following updates at each time interval $t_i$:

$$\left.\begin{aligned} \left\langle \hat{P}_c \right\rangle_i &= \frac{1}{n}\sum_{k=i-n+1}^{i} P_{ck} \\ \hat{P}_{0i} &= \frac{\left\langle \hat{P}_c \right\rangle_i}{1 - \frac{\mu}{h^2}(R^2 + \hat{\mathbf{x}}_i^\mathsf{T}\hat{\mathbf{x}}_i)} \\ \mathbf{z}_i &= P_{ci} - \left\langle \hat{P}_c \right\rangle_i \\ \mathbf{x}_{ai} &= \begin{bmatrix} R\cos(\omega t_i) \\ R\sin(\omega t_i) \end{bmatrix} \\ \mathbf{H}_i &= \frac{2\hat{P}_{0i}\mu}{h^2}\mathbf{x}_{ai}^\mathsf{T} \\ \mathbf{T} &= \begin{bmatrix} \mathbf{R}^{1/2} & \mathbf{H}_i\mathbf{S}_i & \mathbf{0} \\ \mathbf{0} & \mathbf{S}_i & \mathbf{Q}^{1/2} \end{bmatrix} \\ \mathbf{T} \times \mathbf{U}_i &= \begin{bmatrix} \mathbf{V}_i^{1/2} & \mathbf{0} & \mathbf{0} \\ \mathbf{G}_i & \mathbf{S}_{i+1} & \mathbf{0} \end{bmatrix} \\ \mathbf{K}_i &= \mathbf{G}_i\mathbf{V}_i^{-1/2} \\ \mathbf{M}_i &= \mathbf{S}_i\mathbf{S}_i^\mathsf{T} \\ \hat{\mathbf{z}}_i &= \mathbf{H}_i\hat{\mathbf{x}}_i \\ \hat{\mathbf{x}}_{i+1} &= \hat{\mathbf{x}}_i + \mathbf{K}_i(\mathbf{z}_i - \hat{\mathbf{z}}_i) \end{aligned}\right\} \tag{16}$$

Here, $n$ is the number of samples in a complete conscan period. $\mathbf{U}_i$ is an orthogonal transformation that triangularizes $\mathbf{T}$ and may be obtained, for example, using Householder transformations. Quantities such as $\mathbf{R}^{1/2}$ are "matrix square roots" or Cholesky factors. The Kalman filter algorithm is straightforward except for the estimation of the average carrier power, $\left\langle \hat{P}_c \right\rangle_i$, which is computed as a running average of the $n$ most recent outputs from the antenna receiver, and estimation of the maximum carrier power, $\hat{P}_{0i}$, which is computed using Eq. (5). Thus, the Kalman filter requires that at least $n$ measurements have been accumulated before the filter can be started. This results in a delay of a single conscan period before the Kalman filter begins producing estimates. A similar delay also occurs in the FFT algorithm.

## IV. Selection of the Conscan Radius

An algorithm for selecting the conscan radius was developed as part of this study. We again assume a constant target offset $\mathbf{x}_i = \mathbf{x}$. Recall from Eq. (5) that the average carrier power over a conscan period is given by

$$\langle P_c \rangle = P_0 \left(1 - \frac{\mu}{h^2}(\mathbf{x}^\mathsf{T}\mathbf{x} + R^2)\right) \tag{17}$$

Obviously, the average carrier power is maximized for $\mathbf{x} = 0$, which can be attained by repointing the antenna until the conscan center coincides with the target location. However, the best that can be done in practice is to repoint the antenna to place the conscan center at the *estimated* target location $\hat{\mathbf{x}}$. In the newly pointed antenna, the average carrier power becomes

$$\langle P_c \rangle = P_0 \left(1 - \frac{\mu}{h^2}\left((\mathbf{x} - \hat{\mathbf{x}})^\mathsf{T}(\mathbf{x} - \hat{\mathbf{x}}) + R^2\right)\right) \tag{18}$$

and the average-carrier-power expectation, using the definition of $\mathbf{M}$ given in Eq. (11), becomes

$$E\left(\langle P_c \rangle\right) = P_0 \left(1 - \frac{\mu}{h^2}\left(\text{trace}(\mathbf{M}) + R^2\right)\right) \tag{19}$$

A necessary condition for the average power to be maximized is for the expectation of the carrier power given by Eq. (19) to be stationary with respect to $R$; taking a differential and setting it to zero requires

$$\frac{\partial}{\partial R}\text{trace}(\mathbf{M}) = -2R \tag{20}$$

An analytic expression for $\mathbf{M}(R)$ for the Kalman filter would be difficult if not impossible to obtain. In principle it would be possible to propagate $\partial\mathbf{M}/\partial R$ along with the Kalman filter equations, but this more than doubles the number of computations performed at each iteration and excessively complicates the algorithm. Instead we use Eq. (12), developed from FFT principles, as an approximation for $\mathbf{M}$, with the reasoning that this result is an upper bound on $\mathbf{M}$ because it is based on data from only a single conscan period. In this case, solving Eq. (20) yields the optimal conscan radius:

$$R_{opt} = \sqrt[4]{\frac{h^4\sigma_\eta^2}{P_0^2\mu^2 n}} \tag{21}$$

Typically the conscan radius is set to result in 0.1 dB gain loss in the carrier power. The set of parameters summarized in Table 1 yields an optimal conscan radius of $R_{opt} = 1.86$ mdeg for a 34-m antenna. The conscan radius for 0.1-dB gain loss is 5.9 mdeg. This suggests that the conscan radius is currently larger than it needs to be, at least for this set of parameters.

## V. Implementation Details

The behavior of the Kalman filter depends heavily on the selection of the process noise and measurement noise covariances and also on the covariance of the state estimate used to initiate the algorithm. The following criteria are used to select these values.

The measurement noise variance $\mathbf{R}$ is assumed to be provided by the RF receiver. (See [4,5] and other material[3,4] for information.) For the simulations, a model developed elsewhere[5] is used. Though $\mathbf{R}$ is not independent of offset angle, it can be considered to be constant for the small offset angles used during conscan.

The process noise covariance $\mathbf{Q}$ can be established by considering the maximum anticipated drift in the offsets within one sample period. We select

$$\mathbf{Q} = (\text{drift rate} \times \text{sample time})^2\mathbf{I} \tag{22}$$

where $\mathbf{I}$ is the $2 \times 2$ identity matrix. The drift rate used in the simulations is

$$\text{drift rate} = \frac{1}{5} \times \frac{R}{\text{conscan period}} \tag{23}$$

An alternative, which we suggest for implementation, would be to use the reciprocal of the antenna gimbal servo bandwidth.

The initial covariance $\mathbf{M}_0$ of the state estimate is given by the expected uncertainty of the initial target location. This should be based on the known open loop (blind)

[3] M. Aung and S. Stephens, "Statistics of the $P_c/N_0$ Estimator in the Block V Receiver," JPL Interoffice Memorandum 3338-92-089 (internal document), Jet Propulsion Laboratory, Pasadena, California, April 29, 1992.

[4] R. E. Scheid, "Statistical Analysis of the Antenna Carrier Power," JPL Interoffice Memorandum 343-92-1291 (internal document), Jet Propulsion Laboratory, Pasadena, California, October 9, 1992.

[5] Ibid.

pointing performance of the antenna. For the simulations, we assume that the target can be located anywhere within the conscan circle; thus we choose

$$\mathbf{M}_0 = R^2\mathbf{I} \tag{24}$$

## VI. Computer Simulations

The parameters used in the computer simulations are typical for a 34-m DSN antenna operating at Ka-band (32 GHz) and are summarized in Table 1. A random-number generator was used to simulate noise in the carrier power. Each simulation used a different seed to start the random-number generator, which ensures that a reasonable cross section of cases is represented. The Kalman filter estimator was then propagated through the data, starting with a zero initial estimate. For comparison to the existing algorithm, the FFT estimator was also propagated. The FFT estimator is easily distinguished from the Kalman filter because updates are produced only once per conscan period. The simulations were written in Matlab, which allows symbolic manipulation of matrices and vectors within an interpretive programming environment.

The first simulation is shown in Figs. 2–4 and illustrates the convergence of both Kalman filter and FFT estimators to a constant target offset. The simulated carrier power is shown in Fig. 2. The sinusoidal modulation of the carrier power resulting from the nonzero offset is readily apparent. Figure 3 shows the output of the Kalman filter and the FFT estimator. The dashed line on the plot indicates the true target location. The Kalman filter estimator begins by collecting carrier power over a single conscan period so that an estimate of the average carrier power $\langle P_{ci} \rangle$ can be obtained. Propagation of the Kalman filter begins immediately thereafter. Convergence of the estimate is virtually complete within a fraction of a conscan period. The Kalman filter estimates are consistently better than the FFT estimates. In fact, in steady state the standard deviation of the Kalman filter estimates is about one-third that of the FFT estimates.

A measure of the convergence of the Kalman filter is given by the norm of the estimate covariance $\mathbf{M}_i$. Figure 4 shows the time history of $|\mathbf{M}_i|$ and demonstrates that the Kalman filter converges very rapidly at first and then reaches steady state after about 100 sec, or about 3 conscan periods. This is an important observation because it assures us that running the simulations longer will not reveal any different behavior of the algorithm.

In the simulation shown in Fig. 5, the measurement noise has been doubled to investigate the relative sensitivities of the two algorithms to measurement noise. Convergence of the Kalman filter algorithm is changed very little, though close examination reveals a larger amplitude in the high-frequency component of the Kalman filter estimates. Errors in the FFT estimates are pronounced, being roughly doubled when the measurement noise is doubled. As before, the Kalman filter estimates are about three times more accurate than the FFT estimates, as measured by the standard deviations in steady state.

The simulation shown in Fig. 6 shows the ability of both algorithms to successfully estimate a relatively large initial offset. Despite the fact that the initial offset was set at more than three times the conscan radius, both algorithms quickly converge to the correct value. In general, convergence is improved in both algorithms as $R$ grows larger.

In Fig. 7, a data dropout between 100 and 150 sec was simulated. The measurement covariance update and state update steps in the Kalman filter algorithm are not applied for each missing measurement. The most recent estimate is used throughout the dropout period, and then when data become available again, the Kalman filter gracefully continues. Recall that this FFT algorithm is incapable of accommodating missing data, so there is no corresponding plot showing FFT estimates.

The ability of the algorithms to accommodate a drifting parameter is illustrated in Fig. 8. For this simulation, the offset is taken to be a constant drift at a rate of 2 mdeg per 100 sec. Both algorithms successfully track the offset, though they consistently underestimate the offset slightly.

The performance of the algorithms in the presence of a gradually changing maximum carrier power $P_0$ is shown in Fig. 9. In this simulation, the nominal carrier power is increased by 2 percent over each conscan period. The Kalman filter algorithm behaves roughly as before, though some oscillation is apparent in the estimates. Numerical experiments have shown that the amplitude of these oscillations increases with the drift rate $P_0$, but degradation of the Kalman filter estimates is gradual and, in this case, is comparable to the FFT algorithm estimates.

## VII. Summary, Conclusions, and Future Work

A sequential estimator for executing conscan on the DSN antennas has been described. The algorithm, based

on a Kalman filter, has important advantages over the existing FFT algorithm, including better accuracy of the estimates, nearly continuous updates, and the ability to accommodate missing data. It also has many of the desirable properties of the FFT algorithm, particularly robustness and the ability to track large initial offsets. In addition, an algorithm that is used for selecting the optimal conscan radius and is based on maximizing carrier power is proposed. The performance and behavior of the Kalman filter algorithm as compared to the FFT algorithm have been analyzed extensively through computer simulations, which have shown that the Kalman filter algorithm is consistently superior.

Future work on the Kalman filter algorithm should concentrate on a field implementation to demonstrate that it can work as well with real data as it works in an idealized computer simulation.

## References


[1] J. E. Ohlson and M. S. Reid, *Conical-Scan Tracking with the 64-m Diameter Antenna at Goldstone*, Technical Report 32-1605, Jet Propulsion Laboratory, Pasadena, California, October 1, 1976.

[2] A. E. Bryson and Y. Ho, *Applied Optimal Control*, New York: Hemisphere Publishing Corporation, 1975.

[3] M. Verhaegen and P. Van Dooren, "Numerical Aspects of Different Kalman Filter Implementations," *IEEE Transactions on Automation and Control*, vol. AC-31, no. 10, pp. 907–917, October 1986.

[4] T. J. Brunzie, "The Parkes Front-End Controller and Noise-Adding Radiometer," *The Telecommunications and Data Acquisition Progress Report 42-102, vol. April–June 1990*, Jet Propulsion Laboratory, Pasadena, California, pp. 119–137, August 15, 1990.

[5] A. M. Monk, "Carrier-to-Noise Power Estimation for the Block V Receiver," *The Telecommunications and Data Acquisition Progress Report 42-106, vol. April–June 1991*, Jet Propulsion Laboratory, Pasadena, California, pp. 353–363, August 15, 1991.

**Table 1. Selected parameters used in the simulations.**

| Quantity | Value | Description |
|---|---|---|
| $n$ | 32 | Number of samples in a conscan period |
| $t$ | 1 sec | Sample period |
| $\sigma_\eta$ | $5.3 \times 10^{-15}$ W | Standard deviation of $P_0$ |
| $\mathbf{R}$ | $\sigma_\eta^2$ | Measurement covariance |
| $R$ | 5.9 mdeg | Conscan radius for 0.1-dB gain loss |
| $\mathbf{M}_0$ | $R^2\mathbf{I}$ | Starting state covariance |
| $\mathbf{Q}$ | $\left(\frac{R}{5n}\right)^2$ | Process noise covariance |
| $\hat{\mathbf{x}}_0$ | $\begin{bmatrix}0\\0\end{bmatrix}$ | Starting estimate |
| $h$ | 65 mdeg | Half-power beamwidth |
| $P_0$ | $4.14 \times 10^{-13}$ W | Maximum carrier power |

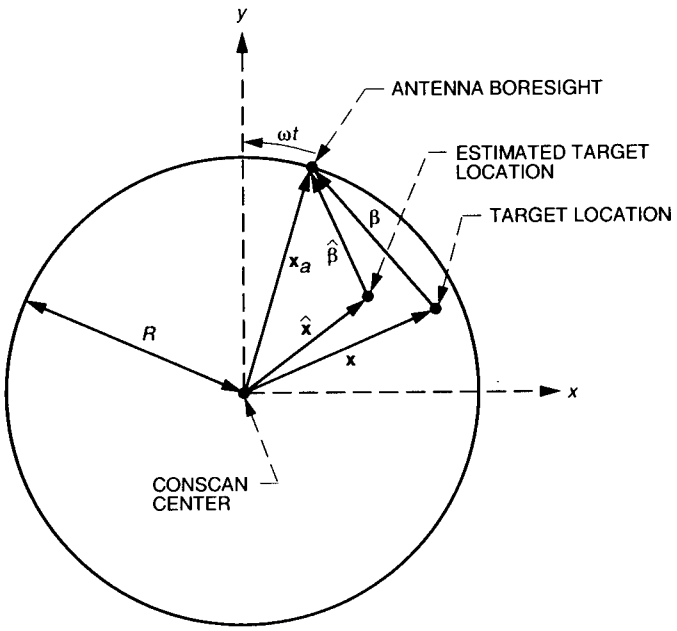


**Fig. 1. Definition of variables.**

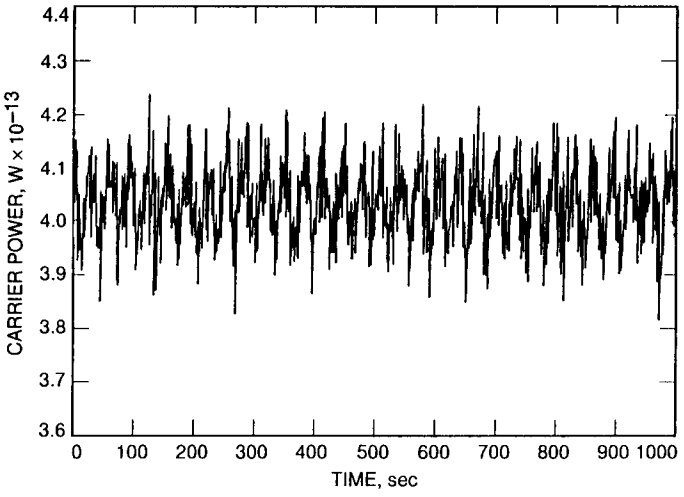


**Fig. 2. Simulated carrier power used for testing conscan algorithms.**

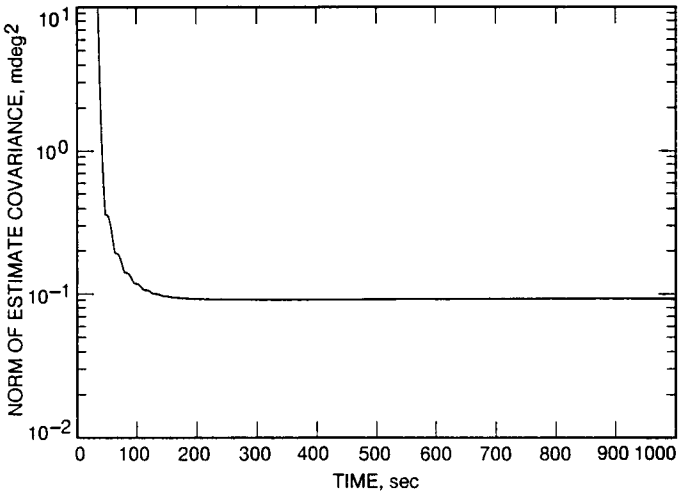


**Fig. 4. Convergence of the estimate covariance for a constant offset.**

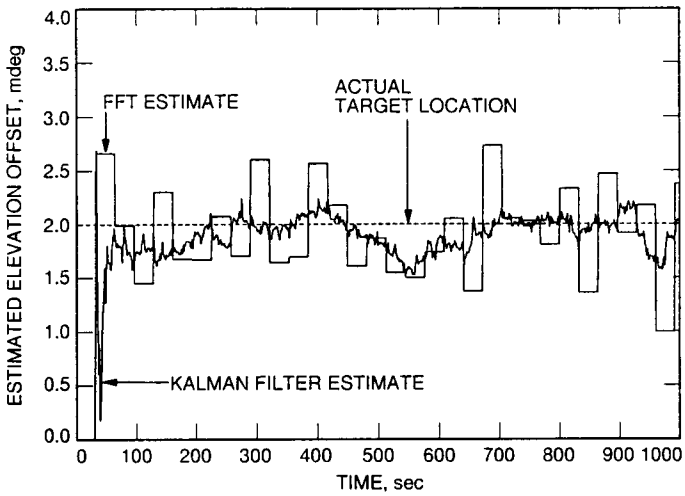


**Fig. 3. Convergence of Kalman filter and FFT estimates to a constant offset.**

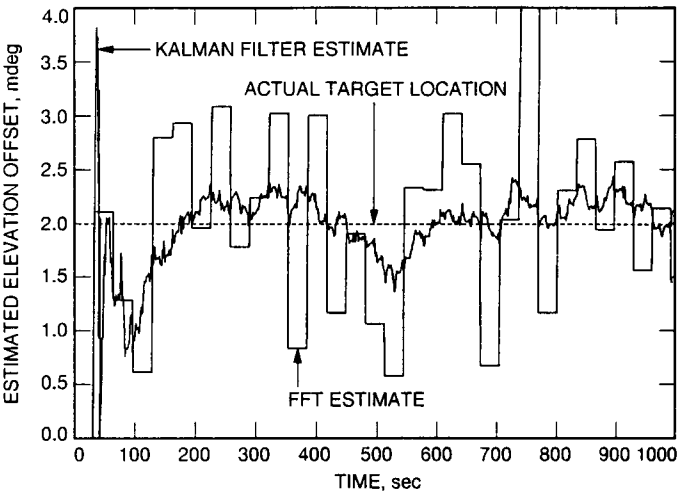


**Fig. 5. Performance of the estimators for doubled measurement noise.**

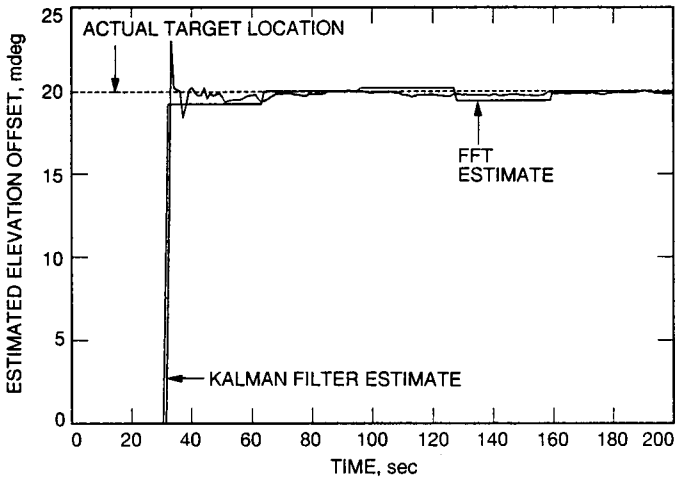


**Fig. 6. Tracking of a large offset.**

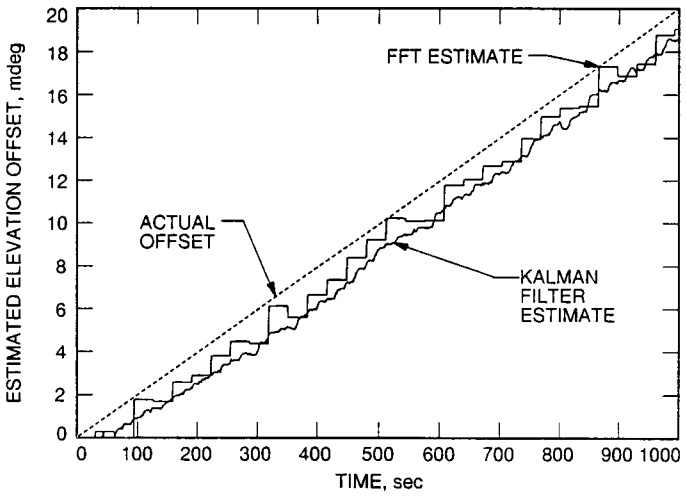


**Fig. 8. Tracking a constant rate drift in the offset.**

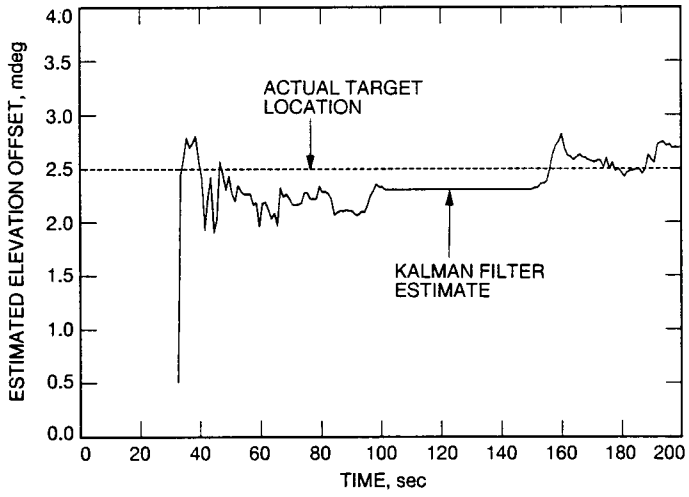


**Fig. 7. Demonstration of the Kalman filter algorithm with a data dropout.**

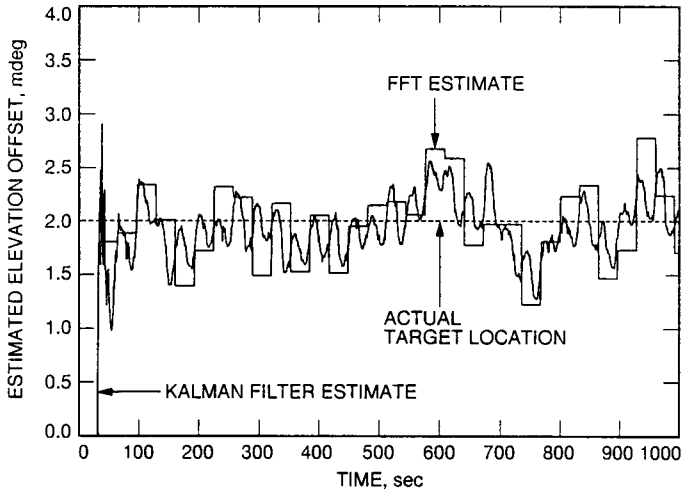


**Fig. 9. Effect of maximum carrier power drift on estimator performance.**